

# Robust Coordinated Tuning of Parameters of Standard Power System Stabilizers for Local and Global Grid Objectives

Bogdan Marinescu, *Member, IEEE*, Badis Mallem, Henri Bourlès, *Member, IEEE*, and Luis Rouco, *Member, IEEE*,

**Abstract**—In this paper we revisit the synthesis of the Power System Stabilizers (PSSs) following some recent objectives and constraints imposed by the evolution of the European interconnected power system. Some principles of approaches used in an independent and even concurrent way are combined and enriched to provide a coordinated way to adjust the parameters of standard (IEEE-type) PSS loops of several machines in a large-scale interconnected system in order to simultaneously reach damping objectives for several oscillatory modes of different natures, i.e., both local and inter-area ones. The trade-off performance/robustness is the central point of the approach since, on the one hand, as the European synchronous zone is being continuously expanded, approximative models should be used in order to keep the size of the problem noncritical from the computational point of view. On the other hand, the increasing size of the system leads to the slipping to lower values of the frequency of the inter-area modes. They are thus further from the local modes which stay at higher frequencies and this makes the coordination of the damping actions for both classes more difficult. Full nonlinear validation simulations are run on a realistic large-scale model of the interconnected European power system.

**Index Terms**—PSS tuning, robustness, coordination.

## I. INTRODUCTION

THE The Power System Stabilizers (PSSs) are additional voltage regulation loops of the generators used to stabilize the behavior of power system. A lot of work has been dedicated to their synthesis. This was traditionally done for local purposes, i.e., to damp the oscillatory modes which involve a limited number of machines close to the studied machine, the so-called *local modes*. Large synchronous zones have also *global* oscillatory phenomena which involve large number of distant machines, characterized by the *inter-area modes* [11]. A new damping objective has then been assigned to the tuning of the PSSs in order to manage *also* the inter-area modes. The latest UCTE interconnection feasibility studies have shown that, with the growth of the European synchronous zone, the frequency of the inter-area modes slips to lower values. This is a new challenge for the tuning of the PSSs since the two classes of modes (local and inter-area

ones) are located in different frequency ranges and thus a careful coordination of the two actions should be achieved.

Since for a large-scale system the damping cannot be achieved by tuning only one PSS, coordination between the tuning actions for different machines has also been envisaged. To achieve this twofold level of coordination, information about the structure of the power system must be used in terms of a *control model* richer than the machine connected to an infinite bus model usually used. For this, in [12] sensitivities of the damping of the studied modes with respect to the gains of the PSSs have been recently used.

Robustness is an important topic in modern control, especially in the case of power systems where, due to the large scale of the problem, the models used for the dynamic studies are a priori simplified. As an example, for the case of feasibility studies of the interconnection of two power systems, the inter-area modes are particularly studied and for this, the small generation units of the system are neglected or aggregated in equivalent ones. This does not affect the global oscillatory behavior of the system, but might have an influence on the local performances of the PSSs when implemented on the real system. Well-established and efficient state-space robust control techniques exist for linear systems (see, e.g., [15]). However, when applied to power systems, the obtained regulators are in state-space form (see, e.g., [3]) and not in the form usually used in practice for the PSSs (like, e.g., the IEEE standard PSS loops [4]). As most of the existing generators are already equipped with those standard PSS structures, to implement such a new regulator, a conversion from the state-space to one of the standard forms is needed [2]. A more direct approach consists in tuning the parameters of a given standard PSS form in order to achieve the desired performances. This leads to a problem of optimization under constraints [5], [6].

In the present paper we investigate the improvement of the robustness and coordination which can be achieved when tuning the parameters of fixed standard PSS structures for several generators in order to simultaneously damp several local and inter-area modes of frequencies within a quite wide range.

The paper is organized as follows: Section II describes the structure of the control model and the way in which its

B. Marinescu and B. Mallem are with Département Méthodes et Ap-pui Réseau de Transport d'Electricité 9, rue de la Porte de Buc, 78000 Versailles, France and SATIE-Ecole Normale Supérieure de Cachan Email: firstname.lastname@rte-france.com.

H. Bourlès is with Conservatoire National des Arts et Métiers 21, rue Pinel, 75013 Paris, France and SATIE-Ecole Normale Supérieure de Cachan Email: henri.bourles@satie.ens-cachan.fr.

L. Rouco is with Instituto de Investigación Tecnológica (IIT), Universidad Pontificia Comillas, Madrid 28015, Spain Email: luis.rouco@iit.upco.es.

parameters are identified. In Section III it is presented the strategy for the tuning of the parameters of the PSS using the control model obtained in Section II. At this stage, stability, robustness and performances of the closed-loop are insured by solving a constrained optimization problem. The influence of the constraints in the PSS synthesis as well as the results provided by this approach are discussed in Section IV via an application to a large-scale representation of the European power system. Section V is devoted to concluding remarks.

## II. CONTROL MODEL

### A. Degrees of detail of the modeling

To synthesize a regulator, a reduced order dynamic model is needed for the system to be controlled. It is called a *control model* and its particularity is to capture only the features which are relevant to the control objectives. The control model most used for the machines of the power systems consists in a machine connected to an infinite bus through a line of variable reactance (see, e.g., [3]). The value of the reactance of this line is used to model the short-circuit power at the grid bus to which the machine is connected. However, doing so, it is difficult to capture both local and inter-area oscillatory phenomena especially when they are of quite different frequencies. To move towards a coordination of tuning of the PSSs for several local and inter-area modes in this new context, sensitivities between the damping of the modes of interest and the gains of the PSSs selected for tuning were used as a control model in [12] as follows : the sensitivity of a closed-loop eigenvalue  $\lambda_i$  with respect to the gain  $K_j$  of the PSS transfer function  $\Gamma_j(s)$  is given by [10]

$$\frac{\partial \lambda_i}{\partial K_j} = r_i^{jj} \quad (1)$$

where  $r_i^{jj}$  is the residue of  $\lambda_i$  in the open-loop transfer function  $H_{jj}(s)$  from  $V_{sj}$  to  $\omega_j$  in Fig. 1.  $V_{sj}$  is the stabilizing signal of the AVR of machine  $j$ , while  $\omega_j$  is the speed of the same machine. Notice also that the transfer mentioned above is computed *before* the installation of the PSSs  $\Gamma_j(s)$ ,  $j = 1, \dots, m$ .

This residue can be computed from the right ( $v_i$ ) and the left ( $w_i$ ) eigenvectors of  $\lambda_i$  and the input ( $B_j$ ), respectively the output ( $C_j$ ) matrices of a minimal state space realization of  $H_{jj}(s)$

$$r_i^{jj} = C_j v_i w_i^T B_j \quad (2)$$

and  $r_i$  is an usual output of softwares for small-signal analysis like, e.g., [13]. From (1) one deduces the impact of small variations of the gain  $K_i$  on the modes of interest:

$$\lambda_i = \lambda_i^0 + r_i K_i \quad (3)$$

where  $\lambda_i^0$  is the mode computed on the open-loop, i.e., the situation in Fig. 1 without  $\Gamma(s)$ .

However, this static characterization can be further enriched to take into account the dynamics of interest of the overall system. Overall dynamic models are usually available for

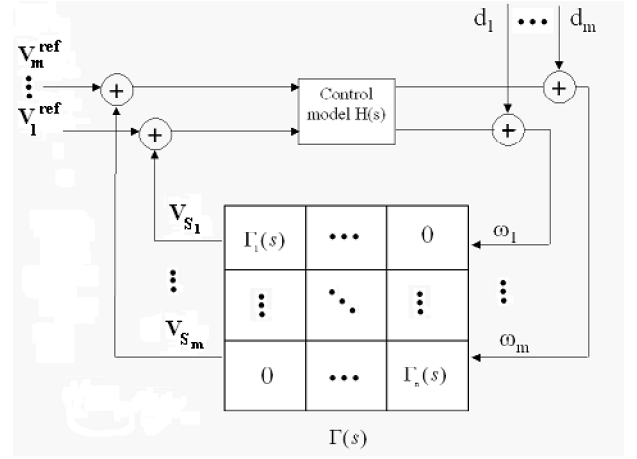


Fig. 1. Control model

the interconnected systems. They consist in a detailed model of the machines of the system of significant installed power (usually the ones of more than 100 MW) along with their regulations and the 400 kV/220 kV transmission grid (see [1] for the case of the European system). Although simplified with respect to reality, this kind of model, called *simulation model* is too complex (about 8000 state variables in the case of the European system) for a control model. It is used for the full nonlinear simulation of the behavior of the power system, in particular for the a posteriori validation of an already synthesized controller. However, it can be used to extract a suitable control model as shown below.

### B. Choice of the control model structure

Let  $\Lambda = \{\lambda_1, \dots, \lambda_l\}$  be the oscillatory modes (local and inter-area) to be damped and  $M = \{M_1, \dots, M_m\}$  the machines for which PSS loops have been chosen to be installed or adapted to perform the damping task. The latter are among the machines with the greatest participation factors [11] in the modes in the set  $\Lambda$  [12].

The control model concerns the power system seen from the PSSs (see Fig. 1), i.e., the transfer matrix  $H(s)$  between the stabilizing signals  $V_s$  of the PSS loops of the machines in the set  $M$  and their speeds:

$$\omega(s) = H(s)V_s(s) \quad (4)$$

where:

$$\omega(s) = \begin{bmatrix} \omega_1(s) \\ \vdots \\ \omega_m(s) \end{bmatrix} \text{ and } V_s(s) = \begin{bmatrix} V_{s1}(s) \\ \vdots \\ V_{sm}(s) \end{bmatrix} \quad (5)$$

This transfer matrix can be made available in practice using a mixed nonlinear/linear analysis framework for power systems like, e.g., [7]. More precisely, the nonlinear system is linearized around a given operation point and, next, the

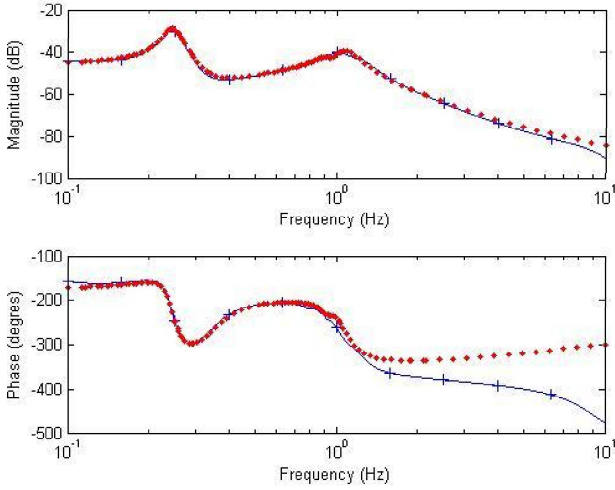


Fig. 2. Bode plots of  $H(s)_{ii}$ ,  $i = PGR$ : Comparison of the full model (blue '+' plot) and the control model (red '.' plot)

frequency response from all the modes can be made available. Bode plots of one entry of  $H(s)$  for the case of the UCTE system are given in Fig. 2. A control model can be obtained from  $H(s)$  if each of its entries  $H_{ij}(s)$  is written as a limited order development plus a correction. Indeed,  $H_{ij}(s) = \sum_{k=1}^n \frac{r_k^{ij}}{s - p_k}$ , where  $r_k^{ij}$  denotes the residue of the pole  $p_k$  of  $H_{ij}$ . Obviously,  $n$ , the total number of poles of  $H$ , is huge since it equals the order of the full simulation model (about 8000 for the European system). However, for the control model, the concerned dynamics are defined within the frequency band of the modes in the set  $\Lambda$ . We propose as control model the following approximation of  $H_{ij}(s)$ ,  $i, j \in \{1, \dots, m\}$ :

$$\tilde{H}_{ij}(s) = \sum_{k=1}^l \left[ \frac{r_k^{ij}}{s - \lambda_k} + \frac{\bar{r}_k^{ij}}{s - \bar{\lambda}_k} \right] + \frac{P(s)}{Q(s)} \quad (6)$$

where  $r_k^{ij}$ ,  $\bar{r}_k^{ij}$ ,  $k = 1, \dots, l$  are known and the polynomials  $P(s)$  and  $Q(s)$  are computed such that  $\tilde{H}_{ij}(s)$  fits  $H(s)_{ij}$  in the frequency working band mentioned above.

### C. Test system

The techniques for the synthesis of the control model and the PSS loops investigated in this paper are tested and illustrated on a realistic large-scale representation of the interconnected European power system which consists of about 400 generators and 2000 buses. The linear model is described by about 8000 state variables. It is well-known that this system exhibits a low damped inter-area oscillation around 0.22 Hz in which the generators of the eastern part of the grid are oscillating against the generators of the western part [1]. This phenomenon is represented by the first two modes of the linearized full model of which dampings are given in the first line of Table I.

They are studied in this paper along with the one in the third column of the same table which is of different nature;

TABLE I  
DAMPING  $\zeta[\%]$  OF THE MODES IN  $\Lambda$

	mode #1 0.23Hz	mode #2 0.24Hz	mode #3 0.91Hz
without PSSs	3.87	11.7	6.25
with PSSs	8.43	9.97	11.53

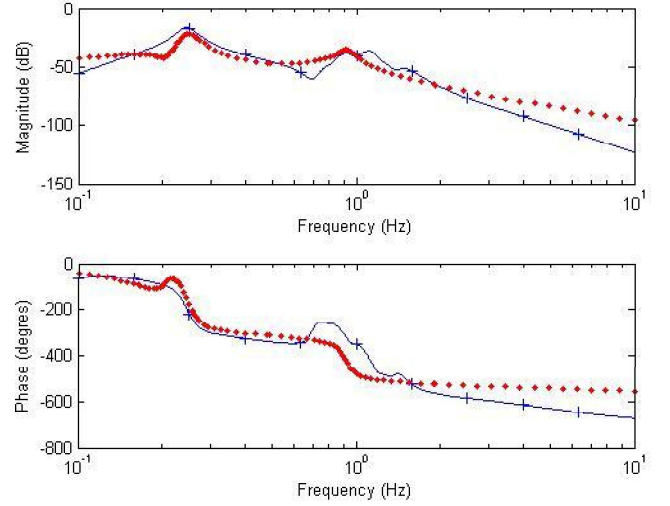


Fig. 3. Bode plots of  $H(s)_{ij}$ ,  $i = Almaraz$ ,  $j = Cofrente$ : Comparison of the full model (blue '+' plot) and the control model (red '.' plot)

it is an inter-area mode of the Spanish system at a slightly higher frequency (0.9 Hz) than the first two ones. Thus, one has (6) with  $l = 3$  and  $\lambda_k$ ,  $k = 1, \dots, 3$  given in Table I.

### D. Frequency identification of the parameters of the control model

The degrees of the polynomials  $P$  and  $Q$  in (3) are chosen such that  $\tilde{H}_{ij}$  is strictly proper:

$$\begin{aligned} Q(s) &= s^v + q_{v-1}s^{v-1} + \dots + q_0 \\ P(s) &= p_{v-1}s^{v-1} + \dots + p_0 \end{aligned} \quad (7)$$

To obtain a control model of order  $2l + v$ ,  $2v$  parameters have to be identified as coefficients of  $P$  and  $Q$ .

If a full simulation model is available for the overall system, the Bode plots of the entries of  $H(s)$  can be easily made available even for the large-scale systems [7].

In Fig. 2 and Fig. 3 such curves are given in solid lines for two transfers of the European interconnected system. They contain information in the wide frequency range of the full simulation model (*i.e.*, about 8000 modes). However, for the stabilization problem we want to solve here, only the frequency range  $[\omega_{\Lambda}^-, \omega_{\Lambda}^+]$  which covers the set of modes  $\Lambda$  is of interest. For the chosen test system, this range is defined around the two major resonance peaks in Fig. 2 and Fig. 3 which correspond to  $\lambda_1$  and  $\lambda_3$  in Table I (the frequency of  $\lambda_2$  is in between), *i.e.*,  $\omega_{\Lambda}^- = 0.15$  Hz,  $\omega_{\Lambda}^+ = 2$  Hz.

An adequate control model should fit the Bode plots of the full simulation model in the frequency range  $[\omega_{\Lambda}^-, \omega_{\Lambda}^+]$ .

The coefficients  $p_i, q_i$  in (7) of each transfer  $\tilde{H}_{ij}(s)$  in (6) are thus computed via a frequency identification procedure based on a least squares objective function of the form

$$J_{ident} = \sum_{\omega_{\Lambda}^- \leq \omega_k \leq \omega_{\Lambda}^+} [\alpha_k (A_k - |\tilde{H}_{ij}(i\omega_k)|)^2 + \beta_k (\varphi_k - \arctan(\tilde{H}_{ij}(i\omega_k)))^2] \quad (8)$$

where  $A_k$  and  $\varphi_k$  are the values of the magnitude and respectively the phase of  $H_{ij}(i\omega_k)$  and  $i^2 = -1$ .  $(A_k, \omega_k)$  and  $(\varphi_k, \omega_k)$  are points of the Bode plots of the transfer of the full simulation model and are thus input data for the frequency identification problem

$$\{p_i, q_i\}_{i \in \{0, \dots, n\}} = \operatorname{argmin}\{J_{ident}\} \quad (9)$$

The weights  $\alpha_k, \beta_k$  are used to manage the trade-off between magnitude and phase fitting and, eventually, to give priority to the fitting at specific frequencies.

A stability constraint on the roots of  $Q$  could be used in (9) to ensure a stable control model  $\tilde{H}_{ij}$  but this is mostly redundant since a low value achieved for  $J_{ident}$  is synonymous of stability of  $Q$  since the full model  $H_{ij}$  is stable.

This identification is repeated as a trial and error iterative procedure with increasing degrees  $n$  for the polynomials above till an acceptable frequency response fitting is achieved.

Such a situation is shown in Fig. 2 for a transfer function of the diagonal of  $H(s)$ . The responses of the full model are in solid lines and the reduced model is obtained with  $\deg(P) = 1$  and  $\deg(Q) = 2$ , i.e., for a control model of order 8. For the transfers of the extra diagonal entries of  $H$  the fitting is more difficult since interactions among different machines should be captured. Fig. 3 shows the result obtained with the same order ( $v = 2$ ) for two Spanish machines ( $i = \text{Almaraz}, j = \text{Cofrentes}$ ). If necessary, accuracy of the identification can be further increased by increasing  $v$ . However, order 2 has been retained for the example treated in this paper since the tuning provided with this model was satisfactory. Indeed, the main objective here is to tune with the simplest control model.

### III. COORDINATED TUNING

The control model (6) is used to simultaneously tune the PSSs of the machines in the set  $M$  for desired target values  $\zeta_i^{ref}, i = 1, \dots, l$  of the damping of the modes in  $\Lambda$ . To ensure a standard IEEE structure for the PSSs, like, e.g.,

$$\frac{V_s(s)}{\omega(s)} = K \frac{1 + T_1 s}{1 + T_2 s} \frac{1 + T_3 s}{1 + T_4 s} \frac{T_5 s}{1 + T_6 s} \quad (10)$$

the problem is formulated as an optimization one which gives an optimal set of gains and time constants for each machine ( $K$  and  $T_i$  in (10)).

#### A. The objective function

The objective function to be minimized should capture the dynamic performance specified, basically the damping of the oscillatory response of the system. In [14] a *modal objective function* is proposed:

$$J_{contr} = \sum_{k=1}^l [(a_k \Psi(\zeta_k, \omega_k) \sum_{i=1}^m \sum_{j=1}^m r_k^{ij} \bar{r}_k^{ij})]^{1/2} \quad (11)$$

$$\Psi(\zeta_k, \omega_k) = \frac{\zeta_k^2 + \omega_k^2}{2\zeta_k^3} (e^{\frac{2\zeta_k^3 T}{\zeta_k^2 + \omega_k^2}} - 1)$$

where  $\zeta_k$  is the damping of the mode  $\lambda_k$ ,  $r_k^{ij}$  is the residue of the same mode in the transfer  $H_{ij}(s)$ ,  $a_k$  a weighting function ( $a_k = 1$  if  $\lambda_k$  is real and  $a_k = 2$  if  $\lambda_k$  is complex) and  $T > 0$  is the time horizon over which  $J_{contr}$  is evaluated.

Roughly speaking, (11) contains the integral of the surface under the modal response envelope through a given time horizon  $T$ . First, the computation of this function is not straightforward in practice and, next, minimizing  $J_{contr}$  given by (11) leads to a response with *maximum* damping which is not necessarily needed. Indeed, only the level  $\zeta_i^{ref}$ ,  $i = 1, \dots, l$  of damping is required and not going below would allow one to settle a better trade-off robustness/performance [15]. This led us to test a simpler and more direct index of performance:

$$J_{contr} = \sum_{i=1}^l (\zeta_i - \zeta_i^{ref})^2 \quad (12)$$

Relation (3) can be exploited to obtain in a simplified manner the influence of the adjustment of the gains of the PSSs on the modes in  $\Lambda$ . Moreover, to reduce the size of the problem, it is considered that  $T_3 = T_1$  and  $T_4 = T_2$  in (10). The optimal PSS parameters are thus:

$$\{K_i^*, T_1^*, T_2^*\} = \operatorname{argmin}_{constraints} \{J_{contr}\} \quad (13)$$

where  $J_{contr}$  is now given by (12).

#### B. The constraints

Several types of constraints are considered:

1) *Physical bound constraints*: They contain the physical bounds for the gains and the time constants of the power system stabilizers (PSSs):

$$\begin{cases} T_{1i} \geq 0 \\ T_{2i} \geq 0 \\ K_i \geq 0 \end{cases}, i \in \{1, \dots, m\} \quad (14)$$

A result with  $K_i^* = 0$  means that the damping objective can be achieved with less PSSs than the a priori chosen family  $M$  (without PSS on machine  $M_i$ ).

An additional upper bound  $K_i \leq K_i^{max}$  can be added to (14) to ensure implementable solutions, i.e., to avoid mathematical solutions with unrealistic high gain.

2) *Stability constraint*: The first nonlinear constraint consists in a stability condition of the resulting closed-loop ( $H(s)$  feedback connected with  $\Gamma(s)$  in Fig. 1). The eigenvalues of state matrix of the closed-loop should be in the left-half plane:

$$\text{Max}\{\text{Re}(\lambda_k^{cl})\} < 0, k \in \{1, \dots, 2l + n + 3m\} \quad (15)$$

Remark that  $\lambda_k^{cl}$  are functions of  $K_i$ ,  $T_{1_i}$  and  $T_{2_i}$  of the PSSs  $\Gamma(s)_i$  of type (10).

3) *Performance/Robustness constraints*: It is well-known in the theory of the robust control (see, e.g., [15]) that the performance and the robustness objectives are contradictory. The result of the tuning of the parameters of the PSSs is thus a trade-off between the two classes of objectives mentioned above. Those objectives can be quantified in terms of  $H^\infty$  norms of some well-chosen transfer matrices of the closed-loop in Fig. 1 which are:

a) *The Sensitivity Function*  $S(s)$  defined by (see [15] for more details)

$$\begin{aligned} \omega(s) &= S(s)d(s) \\ S(s) &= [I_m - \Gamma(s)H(s)]^{-1} \end{aligned} \quad (16)$$

where  $d(s) = \begin{bmatrix} d_1(s) \\ \vdots \\ d_m(s) \end{bmatrix}$  in Fig. 1.

$S(s)$  gives the influence of an additive output disturbance to the output of the system. To ensure a good level of rejection of such type of disturbance one must thus make

$$\|S(s)\|_\infty \leq S^{max} \quad (17)$$

$\|S(s)\|_\infty$  is thus a measure of the *performances* of the closed-loop.

b) *The Complementary Sensitivity Function*  $T(s)$  defined by

$$T(s) = S(s)\Gamma(s)H(s) \quad (18)$$

gives the influence of the output noise to the output  $\omega(s)$  of the closed-loop. To improve the attenuation of the output noise one should thus make

$$\|T(s)\|_\infty \leq T^{max} \quad (19)$$

Also,  $V_s(s) = T(s)V^{ref}(s)$  in Fig. 1. Thus, when minimizing the norm of  $T$ , one minimizes also the energy of the stabilizing signal  $V_s$ , i.e., the level of the control for the problem studied here.  $\|T(s)\|_\infty$  is thus a measure of the *robustness* of the closed-loop and constraints (17) and (19) have opposite effects. By adequate choices of  $S^{max}$  and  $T^{max}$  one can thus manage the trade-off between performances and robustness, well-known in control theory ([15]).

The influence of those constraints on the optimization (13) is discussed on the studied system in the next section.

TABLE II  
EFFECT OF INITIAL VALUES OF PARAMETERS ON THE CONVERGED ONES  
IN CASE OF TWO CHOICES

Machine	$K^*$	$T_1^* = T_2^*$	$T_2^* = T_4^*$
Almaraz	0.0013 / 0	0 / 0.21	0 / 0.23
Cofrente	0.004 / 4.56	0 / 0.49	0 / 0.06
PGR	0.01 / 0	0 / 0.50	0 / 0.06

Problem (13) is a minimization of a nonlinear objective function (3) under mixed linear (14) and nonlinear ((15), (17) and (19)) constraints. It was solved here using the standard Matlab routines (based on the Levenberg-Marquardt algorithm [9]).

#### IV. TESTS AND VALIDATION

For the test system presented in Section II-C, the Spanish machines Almaraz, Cofrentes and PGR were chosen to damp the modes selected in Table I since they have high participation in these modes and they are not already equipped with PSSs. The damping target is  $\zeta^{ref} = 10\%$  for each of the three modes. This objective is interpreted as follows: mode #1 is poorly damped but the damping actions should be chosen in order to not degrade the damping of the other two modes, one directly concerned by the east-west oscillation and the other one local to the Spanish system.

##### A. Influence of the constraints and of the initial point

1) *Initialization*: The choice of the initial point ( $K_i^0, T_i^0$ ) of the optimization (13) is important. Indeed, if a trivial initial point  $K_i^0 = 0, T_i^0 = 0$  is chosen, (13) lacks on a local optimum (for example,  $J_{contr}^* = 0.0045$ ) with less physical meaning (in the treated example, all the time-constants  $T_i^*$  of the solution are zero as indicated in the first entries of Table II). A better way of doing is to start the optimization with  $K_i^0$  computed using (3) with the target poles  $\lambda_i^*$  deduced from the target dampings  $\zeta^{ref}$  and usual values for  $T_i^0$  ( $T_1^0 = 0.2$  s,  $T_2^0 = 0.02$  s). Doing so, a lower value of the performance function is obtained ( $J_{contr}^* = 0.0031$  for the same example treated above) with more realistic parameters for the PSSs (second entries in Table II).

2) *Nonlinear Constraints*: To study the influence of the non linear constraints, the influence of the initialization have been eliminated by using the same initial points for all the tests above. So. Adding constraints of type (17) or (19) obviously increases the difficulty of the optimization problem, i.e., the number of iterations. However, doing so, one can better handle the trade-off robustness/performance or to more precisely assign some specific levels of performance. As an example, when adding (17), as shown in Table III, a better damping is achieved in this case with  $S^{max} = 2$  (values in line 2) in comparison to the case when only the constraints (14) and (15) are used in the optimization (13) (the results in this case are given in line 1 of the same table). Also, as it is shown below, constraint (17) leads also to a better output disturbance rejection.

TABLE III  
EFFECT OF THE IMPOSED CONSTRAINTS INTO ACHIEVED OBJECTIVE FUNCTION, EIGENVALUE DAMPING AND STABILIZER GAIN

Constraints	$\ \zeta^* - \zeta_{ref}\ $	$\zeta_1$	$\zeta_2$	$\zeta_3$	$K_1^*$	$K_2^*$	$K_3^*$
(14) & (15)	0.0019	0.1004	0.0855	0.0583	0	4.56	0
(14) & (15) & (17)	0.0018	0.1005	0.0907	0.0583	0.59	4.81	0
(14) & (15) & (19)	0.0021	0.0952	0.0800	0.0587	0	3.55	0.008

TABLE IV  
COMPARISON OF THE STABILIZER PARAMETERS ACHIEVED WITH COORDINATED TUNING AND WITH ROBUST COORDINATED TUNING

	$K^*$	$T_1^* = T_3^*$	$T_2^* = T_4^*$
Almaraz	0.59 / 2.43	0.22 / 0.21	0.05 / 0.02
Cofrente	4.81 / 5.74	0.59 / 0.58	0.15 / 0.05
PGR	0 / 0.54	0.71 / 0.61	0.15 / 0.06

On the contrary, constraint (19) has the opposite effect. As explained in Section III-B3, when including (19), the damping is lower (line 3 in Table III obtained for  $T^{max} = 1.2$ ) but the energy of the control is lower and thus, the robustness is improved. Indeed, in this case  $\|V_s(s)\|_2^2 = 1.48$  while  $\|V_s(s)\|_2^2 = 1.91$  for the control generated only with the constraints (14) and (15) (PSS parameters in line 1 of Table III).

### B. Linear validation

For a more functional validation, the results obtained minimizing (13) under the constraints (14), (15) and (17) with  $S^{max} = 2$  (parameters given in line 2 of Table I and first positions of the entries in Table IV) are compared to the ones provided by the tuning proposed in [12] where only a static control model is used (second position in the same Table IV). First, the gains obtained with the procedure presented above are lower than the ones in [12] and thus the robustness is improved in general. This difference can also be remarked in the Bode plots of the open-loop transfer functions of the control system, i.e.,  $\Gamma_i H_{ii}$ , given in Fig. 4 for  $i = \text{Almaraz}$ . Next, only two machines (Almaraz and Cofrentes) are needed to reach the damping objectives with the tuning procedure presented here since the gain obtained for PGR is  $K^* = 0$  as shown by the damping values in line 2 of Table I.

With the present synthesis, also the disturbances on the machine speed are better rejected as seen in Fig. 5 which comparatively presents the linear closed-loop responses of  $\omega$  of the Almaraz machine at an unitary step additive disturbance ( $d$  in Fig. 1) on the output of the same machine.

### C. Full nonlinear validation

The achieved level of performance evaluated on the linear model is given in Table I. It is now shown that this level is still valid in nonlinear simulation. For the latter validation, the system is simulated in detail using the Eurostag software for transient stability analysis [8]. All the machines of the overall model (about 800 representative machines of the European power system) along with their detailed regulations and the 225 kV/400 kV grid transmission system are taken into

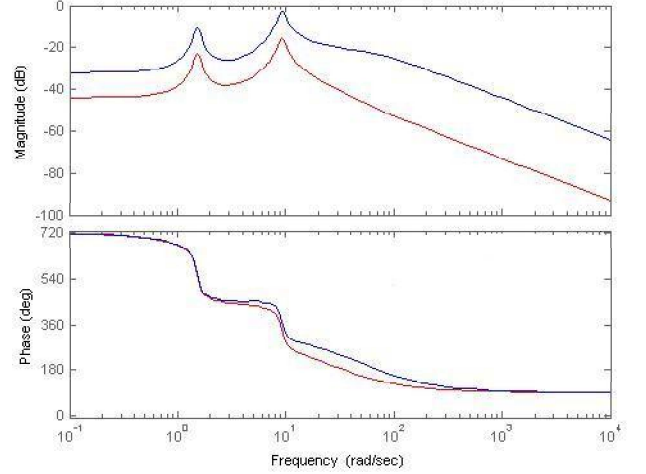


Fig. 4. Bode plots of  $\Gamma_i H_{ii}$ ,  $i = \text{Almaraz}$

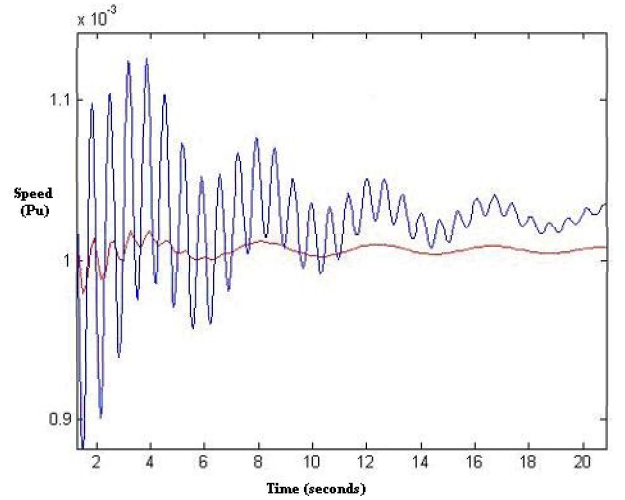


Fig. 5. Output disturbance rejection: Comparison of the Coordinated tuning model (blue plot) and Robust coordinated tuning model (red plot)

account in a precise electromechanic nonlinear modeling. Fig. 6 gives the speed responses of machines Almaraz to a short-circuit of 200ms at the grid connection point of the same machine. It can be seen that the damping of the response is improved (the more damped curve corresponds to the situation when the 2 PSSs described in the first entries of Table IV) are used, while the less damped response is obtained on the initial situation when no PSSs are used on the machines in the set  $M$ ).



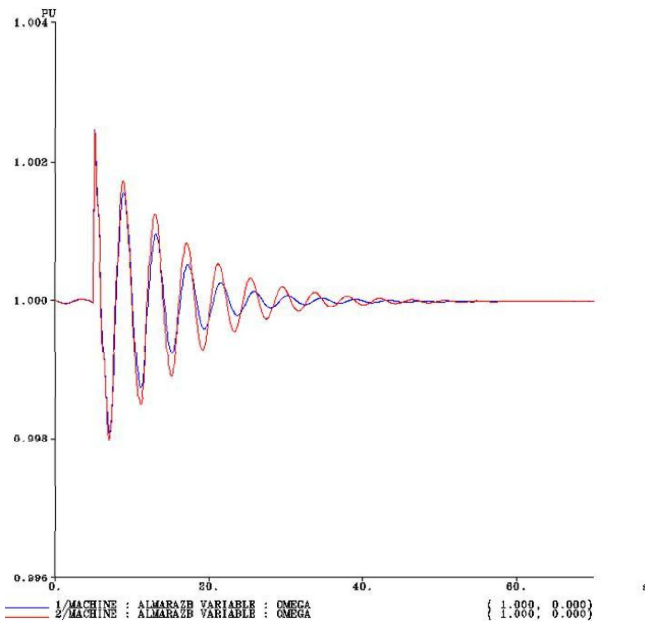


Fig. 6. Nonlinear simulation

## V. CONCLUDING REMARKS

The use of a dynamic control model allows coordination in fulfilling local and global damping objectives. Robustness techniques of modern control theory can be used with the constraint of keeping an a priori given structure of the PSS loops. This is a promising track to tackle the new requirements of the evolving European system in which the inter-area modes are at lower frequencies, thus further from the local ones and closer to the turbine dynamics with which the PSSs loops may now interact.

## ACKNOWLEDGMENT

The authors would like to thank Mr. S. Henry, Head of the group FDS at RTE-France for helpful remarks.

## REFERENCES

- [1] H. Breulmann et al., "Analysis and Damping of Inter-area Oscillations in the UCTE-CENTREL Power-System", *CIGRE Session*, Paper 38-113, Paris, 2000.
- [2] A. Elices, L. Rouco, H. Bourlès and T. Margotin, "Conversion of State Feedback Controllers to the Standard AVR+PSS Form", *Proc. IEEE PowerTech Conference*, Bologna-Italy, June 2003.
- [3] A. Elices, L. Rouco, H. Bourlès and T. Margotin, "Design of Robust Controllers for Damping Inter-area Oscillations: Application to the European Power Systems", *IEEE Trans. on Power Systems*, vol. 19, no. 2, May 2004, pp. 1058-1067.
- [4] IEEE Power Engineering Society, "IEEE Recommended Practice for Excitation System Models for Power System Stability Studies", *IEEE Std. 421.5*, 2005.
- [5] I. Kamwa, G. Trudel and D. Lefebvre, "Optimization-Based Tuning and Coordination of Flexible Damping Controllers for Bulk Power Systems", *Proc. IEEE International Conference on Control Applications*, August 1999.
- [6] I. Kamwa, G. Trudel and L.Gérin-Lajoie, "Robust Design and Coordination of Multiple Damping Controllers Using Nonlinear Constraints Optimization", *Proc. PICA*, 1999.
- [7] B. Marinescu and L. Rouco, "A Unified Framework for Nonlinear Dynamic Simulation and Modal Analysis for Control of Large-Scale Power Systems", *Proc. Power Systems Computations Conference*, Liège-Belgium, August 2005.

- [8] B. Meyer and M. Stubbe, "Eurostag, a Single Tool for Power System Simulation", *Proc. of IEEE Conf. on Transmission and Distribution*, March 1992.
- [9] J.J. More, "The levenberg-Marquardt: Implementation and Theory", *Numerical Analysis*, ed. G.A. Watson, Lecture Notes in Mathematics 630, Springer-Verlag, pp. 105-116, 1977.
- [10] G.N. Taranto, A.L.B. do Bomfim, D.M. Falcao, N. Martins, S. Gomes, P.E. Quintao, "Combined use of Analytic and Genetic Algorithms for Robust Coordinated Tuning of Power System Damping Controllers", *Proc. of the Bulk Power System Dynamics and Control IV-Restructuring Conference*, August 24-28, Santorini (Greece), 1998.
- [11] G. Rogers, *Power System Oscillations*, Norwell, MA: Kluwer, 2000.
- [12] L. Rouco, "Coordinated Design of Multiple Controllers for Damping Power System Oscillations", *International Journal of Electrical Power and Energy Systems*, Vol.23, No.7, pp. 517-530, October 2001.
- [13] L. Rouco, I.J. Prez-Arriaga, R. Criado and J. Soto, "A computer Package for Analysis of Small Signal Stability in Large Electric Power Systems", *Proceedings of the 11th Power Systems Computations Conference*, pp. 1141-1148, Avignon (France), August 1993.
- [14] J.B. Simo, I. Kamwa, G. Trudel and S.-A. Tahan, "Validation of a new modal performance measure for flexible controllers design", *IEEE Trans. on Power Systems*, vol. 11, no. 2, May 1996.
- [15] S. Skogestad and I. Postlethwaite, *Multivariable Feedback Control*, John Wiley and Sons Ltd., Chichester-England, 1996.